International Journal of Pharmaceutics 616 (2022) 121524

Contents lists available at ScienceDirect

International Journal of Pharmaceutics

journal homepage: www.elsevier.com/locate/ijpharm

Potential use for chronic pain: Poly(Ethylene Glycol)-Poly (Lactic-Co-Glycolic Acid) nanoparticles enhance the effects of Cannabis-Based terpenes on calcium influx in TRPV1-Expressing cells

Mazen M. El-Hammadi [a], Andrea L. Small-Howard [b], Chad Jansen [c], Mercedes Fernández-Arévalo [a], Helen Turner [c], Lucía Martín-Banderas [a,d,*]

[a] Departmento de Farmacia y Tecnología Farmacéutica, Facultad de Farmacia, Universidad de Sevilla, c/Prof. García González n°2, 41012, Sevilla, Spain
[b] Gb Sciences, Inc. (OTCQB:GBLX), 3550 W. Teco Avenue, Las Vegas, NV, USA
[c] Laboratory of Immunology and Signal Transduction, Chaminade University of Honolulu, 3140 Waialae Avenue, Honolulu, HI 96816, USA
[d] Instituto de Biomedicina de Sevilla (IBiS), Hospital Universitario Virgen del Rocio/CSIC/Universidad de Sevilla, Seville, Spain

ARTICLE INFO

Keywords:
Cannabis-based terpenes
PLGA polymeric nanoparticles
Beta-myrcene
Nerolidol
Beta-caryophyllene
Nanomedicine
Chronic pain

ABSTRACT

The objective of these *in vitro* studies was to investigate the impact of the encapsulation of three cannabis-based terpenes, namely β-myrcene (MC), β-caryophyllene (CPh), and nerolidol (NL), on their potential efficacy in pain management. Terpene-encapsulated poly(ethylene glycol)-poly(lactic-co-glycolic acid) nanoparticles (PEG-PLGA NPs) were prepared by an emulsion-solvent evaporation method. The terpene-loaded NPs were examined in HEK293 cells that express the nociceptive transient receptor potential vanilloid- 1 (TRPV1), an ion channel involved in pain perception. TRPV1 activation was assessed by monitoring calcium influx kinetics over 1 h in cells pre-treated with the fluorescent indicator Fluo-4. In addition, the fluorescence intensity changes induced by the NPs in living cells were also explored by a fluorescence microscope. Furthermore, the cytotoxicity of the terpene-loaded NPs was evaluated by the 3-(4,5-dimethylthiazol-2-yl)-3,5-diphenyl tetrazolium bromide (MTT) proliferation assay. The terpene-loaded NPs had a diameter in the range of 250–350 nm and a zeta potential of approximately −20 mV. The encapsulation efficiency was 18.5%, 51.3%, and 60.3% for MC, NL, and CPh NPs, respectively. The nano-formulations significantly increased the fluorescence intensity in comparison with free terpenes. Furthermore, combinations of terpene-loaded NPs produced significantly higher calcium responses when compared to combinations of free terpenes. Similar findings were shown by the fluorescence images. In conclusion, the terpene-PLGA NPs can be promising therapeutics for more effective pain management.

1. Introduction

Cannabis has been employed in medicine for millennia, particularly in pain management. In the last two decades and owing to serious adverse effects associated with the use of opiate medications and non-steroidal anti-inflammatory drugs (NSAIDs), the two major pharmacological groups used in pain management, more attention has been paid to cannabis-based extracts and cannabinoid-based products to fill the gap left by analgesics currently available in the clinic (Romero-Sandoval et al., 2018). Increasing evidence from human clinical trials has demonstrated that cannabis-based therapeutics can minimize neuropathic pain intensity and provide effective remedies for chronic pain management (Maharajan et al., 2020). However, the clinical use of herbal cannabis is opposed by several limitations including the psychoactive adverse effects (related to Δ9-tetrahydrocannabinol, THC) and associated harm to individuals and the public health, the complex and variable chemical content with the associated lack of consistency and standardization, possible microbial and pesticidal contamination, as well as the lack of solid evidence of effectiveness. Therefore, there is a critical need for robust research on herbal cannabis and its ingredients to evaluate the medical potential of the active ingredients alone and in complex mixtures (Bridgeman and Abazia, 2017; Brunetti et al., 2020). Potentially bioactive cannabis-derived compounds not only include cannabinoids but also terpenes, which comprise more than 150

* Corresponding author at: Departmento de Farmacia y Tecnología Farmac éutica, Facultad de Farmacia, Universidad de Sevilla, c/Prof. Garc ía Gonz ález n °2, 41012, Sevilla, Spain.
E-mail addresses: mazenhammadi@us.es (M.M. El-Hammadi), luciamartin@us.es (L. Martín-Banderas).

https://doi.org/10.1016/j.ijpharm.2022.121524
Received 3 November 2021; Received in revised form 10 January 2022; Accepted 25 January 2022
Available online 30 January 2022

compounds out of the 500 plus constituents of *Cannabis Sativa*, the most commonly used cannabis species (Booth and Bohlmann, 2019). Based on the fact that different cannabis varieties are able to induce various physiological effects, as has been observed among cannabis users, the so-called "entourage effect" has been proposed to refer to the additive or synergistic contribution of terpenes to the pharmacological effects shown by cannabinoids (Russo, 2011).

In a recent study that investigated the ability of terpenes found in *C. Sativa* to activate TRPV1 in HEK cells, a mixture of terpenes was found to remarkably promote intracellular calcium influxes. In addition, *beta*-myrcene (MC) and, to a lesser extent, nerolidol (NL) were identified as the major contributors to the calcium influx activity. MC activity was completely dependent upon the presence of TRPV1 protein and thus the TRPV1 antagonist capsazeine could effectively bloke MC-induced calcium influx. Furthermore, based on molecular docking data, MC binds to TRPV1 to via a hydrophobic, non-covalent interaction (Jansen et al., 2019).

MC (Fig. 1-A), a monoterpene and the most abundant terpene in cannabis, and NL (Fig. 1-C,D), a sesquiterpene, have both demonstrated anti-nociceptive and anti-inflammatory effects (Burcu et al., 2016; Chan et al., 2016; Ciftci et al., 2014). In addition to these two terpenes, *beta*-caryophyllene (CPh) (Fig. 1-B), a bicyclic sesquiterpene found in cannabis, has been reported to act as a specific agonist against cannabinoid receptor 2 (CB2), which presents in peripheral organs, outside the CNS (Chicca et al., 2014). This interesting activity, beside other mechanisms of action, make CPh a potential therapeutic candidate in the management of neuropathic pain (Sharma et al., 2016). However, the volatile and hydrophobic nature of these terpenes result in poor solubility and low bioavailability, limiting their *in vivo* pharmacological efficacy. To address these limitations, we have recently developed polymeric nanoparticles (NP) that successfully encapsulated these three terpenes (El-Hammadi et al., 2021; Small-Howard et al., 2019). The new nanosystems were fabricated using poly(ethylene glycol)-poly(lactide-co-glycolide) (PEG-PLGA), a block co-polymer of a hydrophilic chain

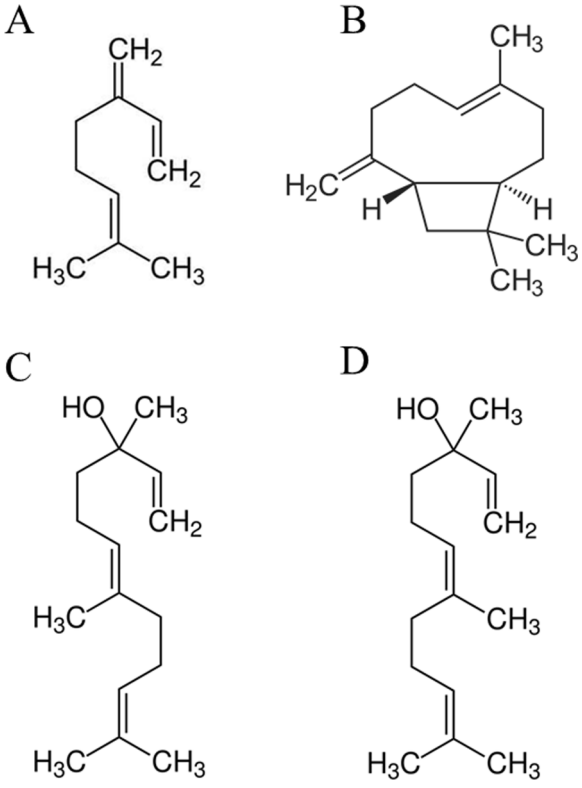

Fig. 1. Structural formulas of (A) β-myrcene, (B) β-caryophyllene, (C) *trans*-nerolidol, and (D) *cis*-nerolidol.

of PEG linked to PLGA a biocompatible, biodegradable, Food and Drug Administration (FDA)-approved co-polymer based (Berrocoso et al., 2017; El-Hammadi and Arias, 2015). It is anticipated that the encapsulation of the cannabis-derived terpenes in PLGA NPs will equip them with a wide range of qualities such as enhanced solubility and stability, promoted absorption by biological membranes, sustained release, and ultimately improved therapeutic efficacy (Han et al., 2012; Iannitelli et al., 2011; Marongiu et al., 2014).

In this work we sought to study the impact of the of MC, CPh, and NL encapsulation on their potential effectiveness in pain management. To this end, we tested the terpene-loaded PEG-PLGA NPs in HEK293 cells (Human Embryonic Kidney cells) that express the nociceptive transient receptor potential vanilloid- 1 ion channel (TRPV1), a non-selective ligand-gated cation channel that is involved in the sensation of scalding heat and pain (Bujak et al., 2019). This ion channel is a member of the TRPV subfamily of the transient receptor potential (TRP) channels, a family of membrane calcium channels that are activated by a variety of exogenous and endogenous physical and chemical stimuli (Huang et al., 2020; So et al., 2020). TRPV1 is identified by its responsiveness to capsaicin and its analogues (like resiniferatoxin), but TRPV1 also responds to noxious temperatures (greater than42 °C), low pH (<5.2), and to some endogenous compounds; in particular, the endocannabinoids (e.g anandamide) (Yang and Zheng, 2017; Zheng and Wen, 2019). TRPV1 antagonists include capsazepine and ruthenium red (Bautista and Julius, 2008; Zhai et al., 2020). TRPV1 is expressed in both peripheral and central nervous systems, predominantly in primary sensory neurons involved in pain perception, in addition to several non-neuronal cells such as immune cells and smooth muscle cells (Molinas et al., 2019). Both antagonism and agonism of TRPV1, and other TRP channels, can induce analgesia, via inactivation and chronic desensitization of this nociceptive ion channel making it a target for pain treatment (Jara-Oseguera et al., 2008). The activation of TRPV1 leads to an influx of Ca^{2+} via the plasma membrane, thus generating changes in intracellular Ca^{2+} concentration. It was also found that TRP channels are present in intracellular organelles and control the release of intracellular Ca^{2+} (Zhai et al., 2020). Influxes of Ca^{2+} were monitored by the fluorescent indicator Fluo-4 acetoxymethyl (AM) (Gee et al., 2000). We used similar experimental conditions to acquire fluorescence images of cells treated with the terpenes-loaded NPs. Additionally, the cytotoxicity of the free and encapsulated terpenes was assessed.

2. Materials

MC, CPh, and NL (a mixture of *cis*- and *trans*-isomers) were provided by Gb Sciences (NV, USA). Polyvinyl alcohol (PVA) 72,000 and the solvents were obtained Panreac Química (Spain). PEG-PLGA (PEG average Mn 2,000, PLGA average Mn 11,500; lactide:glycolide 50:50), and all other chemicals were purchased from Merck (Germany), and were of analytical quality. Water used in the experiments was deionized and filtered (Milli-Q Advantage A10, Millipore, Spain).

3. Methods

3.1. Preparation of nanoparticles

Terpene-encapsulated PEG-PLGA NPs were prepared by an emulsion-solvent evaporation method, as previously described (El-Hammadi et al., 2021). Briefly, an organic phase containing 10 mg of MC, CPh, or NL and 40 mg of PEG-PLGA dissolved in 1 mL ethyl acetate (EA), was added dropwise to 5 mL of PVA aqueous solution (0.5% w/v) under vigorous mixing using a high-speed homogenizer (Polytron® PT 2500 E, Kinematica AG, Switzerland) for 60 sec. The organic solvent was then removed using a rotary evaporator, and NPs were collected by ultra-filtration (Amicon® tubes Ultracel-100 kDa regenerated cellulose membrane, 15 mL sample volume) at 4,000 × *g* at 12 °C. Finally, NPs dispersed in 5% (w/v) trehalose, were lyophilized (-80 °C, <0.100 mbar;

TELSTAR Cryodos, Spain) and collected as white cotton-like material.

3.1.1. Nps characterization

Mean diameter and zeta potential of the produced NPs were determined by dynamic light scattering and laser Doppler electrophoresis (Nanosizer ZS, Malvern Instruments Ltd., UK), respectively. NPs were diluted with MQ water to around 1 mg/ml before measurements.

3.1.2. Measurement of terpene load capacity

The encapsulated terpene in the resulting NPs were measured using a GC–MS method, as previously described (El-Hammadi et al., 2021). Briefly, encapsulated terpenes extracted from the lyophilized NPs and dissolved in dichloromethane (DCM) were analyzed using a trace gas chromatography system in tandem with a mass spectrometer (DELTA V™ Isotope Ratio Mass Spectrometer, Thermo Scientific, USA). Data acquisition and analyses were performed using Xcalibur 2.0.7 (Thermo Scientific, USA). A SPB-1 capillary GC column (30 m × 0.25 mm × 1.5 µm, Sigma-Aldrich, USA) was employed. Analyses were run for 15 min and the peaks of MC, CPh, *cis*-NL, and *trans*-NL were observed at a retention time of 6.92, 5.73, 6.77, and 7.16 min, respectively. For mass spectrometry detection, ionization was carried out by electronic impact (EI) with a full scan mode in the *m/z* range of 20–300 and an ion source temperature of 250 °C in positive ion mode. For quantification purposes, the characteristic ions for terpenes at *m/z* 69, 93 and 133 were monitored by selected ion monitoring (SIM) mode.

3.1.3. Terpene loading and entrapment efficiency

Terpene content is expressed as entrapment efficiency (EE, %) and drug loading (DL, %) following the equations 1 and 2, respectively:

$$\text{EE}\ (\%) = \frac{\text{mass of terpene incorporated (mg)}}{\text{initial mass of terpene (mg)}} \times 100 \quad (1)$$

$$\text{DL}\ (\%) = \frac{\text{mass of terpene incorporated (mg)}}{\text{initial mass of nanocarrier (mg)}} \times 100 \quad (2)$$

3.2. In vitro experiments

3.2.1. Cell maintenance

HEK TRPV1 cells were provided by Dr. Helen Turner's lab at Chaminade University in Honolulu, Hawai'i (USA). Cells were maintained in MEM essential medium (Corning, NY, USA) supplemented with 10% FBS, 50 units/ml-50 µg/ml penicillin–streptomycin (Sigma-Aldrich (USA), and 0.6 mg/ml geneticin (Gibco AG, Basel, Switzerland), in a humidified atmosphere with 5% CO_2 at 37°C.

3.2.2. In vitro cytotoxicity

The cytotoxicity of the terpene-loaded NPs was evaluated by the 3-(4,5-dimethylthiazol-2-yl)-3,5-diphenyl tetrazolium bromide (MTT) proliferation assay, determining mitochondrial dehydrogenase activity. Cells were seeded in monolayer culture into 96-well plates (3×10^4 cells/well) and incubated overnight at 37 °C in air with 5% CO_2. Various concentrations of free terpenes, terpene-loaded NPs, and blank NPs (dilutions like that of the terpene-loaded particles used in these tests) were added to the cells in the culture medium. After 24 h of incubation at 37.0 ± 0.5 °C, the culture medium was removed and replaced with 200 µl of MTT solution (0.5 mg/mL in cell culture medium). The medium was removed after incubation for 4 h at this temperature, and 200 µl of DMSO was added to each well to dissolve the resultant formazan crystals. Untreated cells and cells treated with Triton × 1% served as controls. Finally, the optical density (OD) at 570 nm was determined using a microplate reader (Synergy HT, BioTek Instruments, Inc., Vermont USA). The relative cell viability (%) was calculated as [(OD treated cells/OD control (untreated) cells) × 100].

3.2.3. Calcium signaling assay

This method can be employed to evaluate the cytosolic concentration of calcium ions, in which the non-fluorescent Fluo 4-acetoxymethyl ester (Fluo-4 AM; Thermos Fisher Scientific) is cleaved by intracellular esterase to form the free green fluorescent Fluo 4, which is a calcium indicator. When it forms a complex with calcium, excitation by light at a wavelength of 488 nm produces marked green fluorescence inside the cell.

3.2.3.1. Assay procedure. HEK TRPV1 cells were harvested with trypsin, deactivated with media, centrifuged at 1000 rpm, for 5 min, at room temperature, and counted. Next, cells were washed twice with 1 mM Ca Assay Buffer (Na Ringers [140 mM NaCl, 2.8 mM KCl, 2 mM $MgCl_2$, 11 mM glucose, 10 mM HEPES], 2 mM Probenecid, 1 mM $CaCl_2$; pH 7.4), and collected by centrifugation at 1000 rpm, for 5 min, at room temperature. Cells were re-suspended in 1 µM Fluo-4 AM (1 µl of 5 mM Fluo-4 AM was mixed with 1 µl of 20% Pluronic F-127 in DMSO, then 5 mL of 1 mM Ca Assay Buffer was added and the mixture incubated for 10 min at 37 °C in the dark). Next, suspended cells were incubated for 30 min at 37 °C in the dark. Cells were then washed twice with 1 mM Ca Assay Buffer, then re-suspended in the assay buffer and pipetted to opaque-walled 96-well plates at a density of 15×10^4 cells/180 µl/well. Fluorescence was measured using a plate reader (Synergy HTX, BioTek, USA), at an excitation/emission wavelengths of 485 nm and of 528 nm, respectively. Once a baseline was established (3 measurements), 20 µl of the stimulant (free terpenes, terpene-loaded NPs, and controls) solution was added to each well and measurement was continued for 1 h at a rate of one read every 40 sec.

3.2.3.2. Preparation of stimulant solutions/dispersions. All solutions/dispersions were prepared in 1 mM Ca Assay Buffer. Free terpenes were first dissolved in DMSO, then a specific volume was diluted with the assay buffer to produce the required concentration. The use of ethanol to dissolve the terpenes was avoided as it can potentiate the response of TRPV1 to stimulants (Moriello and De Petrocellis, 2016). Terpene-loaded PEG-PLGA NPs were diluted directly using the assay buffer. Negative controls of assay buffer containing DMSO and blank NPs were also prepared. Ionomycin 4 µM was used as a positive control. Ionomycin is a calcium ionophore that increases the intracellular concentration of Ca^{2+}, $[Ca^{2+}]i$, by facilitating its transport across the plasma membrane. Free and encapsulated terpenes were prepared at a concentration of 400 µg/ml (to give a final concentration of 40 µg/ml after addition to the cells) either as individual terpenes, or in combinations with other terpenes (MC/NL, NC/CPh, NL/CPh, or MC/NL/CPh). Responses of negative controls were deducted, and averages were computed and used to plot the calcium responses profiles.

3.2.4. Fluorescence imaging – Image acquiring and analysis

3.2.4.1. Assay procedure. The ability of terpenes loaded PEG-PLGA NPs to modulate calcium flux in HEK TRPV1 cells was also examined by evaluating intercellular fluorescence intensity, using Fluo-4 AM, under a fluorescence microscope. In this experiment, HEK TRPV1 cells were seeded in 96-well cell culture plates (3×10^4 cells/well; each well received 200 µl of cell suspension). The plates were incubated for 48 h at 37 °C in air with 5% CO_2. On treatment day, cells were washed twice with 1 mM Ca Assay Buffer. To each well, 100 µl of the green-fluorescent calcium indicator Fluo-4 (1 µM; 1 µl of 5 mM Fluo-4, mixed with 1 µl of 20% Pluronic F-127 in DMSO, then 5 mL of 1 mM Ca Assay Buffer was added and the mixture incubated at 37 °C for 10 min in the dark) was pipetted and plates were incubated for 30 min at 37 °C in the dark. Cells were washed twice with 1 mM Ca Assay Buffer, then 180 µl of 1 mM Ca Assay Buffer was added to each well prior to treatment.

3.2.4.2. Preparation of stimulant solutions/dispersions. Stimulant

solutions/dispersions were prepared using the same procedure under Calcium Signaling Assay. Free and encapsulated terpenes were prepared at a concentration of 400 μg/ml (in 1 mM Ca Assay Buffer) of each terpene either as single terpenes or in combinations.

3.2.4.3. Treatment and imaging. Volumes of 20 μl of previously prepared simulants and controls were added to wells (a total volume of 200 μl per well; 20 μl stimulant/control + 180 μl buffer). The final concentration of each terpene in all treatments was 40 μg/ml, thus a total concentration of 40, 80 or 120 μg/ml of terpenes was used in single (MC, CPh, and NL), double (MC/NL, MC/CPh, NL/CPh) and triple (MC/CPh/NL) preparations, respectively.

The intensity of intracellular green fluorescence was observed using Nikon inverted microscope Eclipse Ti (Japan). Images of live cells were acquired 30 min and 60 min post treatment (exposure settings: exposure 1 s, gain 7.6×; emission wavelength: 470 nm /FITC filter).

3.2.4.4. Analysis of images. The acquired images were analyzed using ImageJ software (Version 1.52r; NIH, USA). The fluorescence intensity was computed using the following equation:

$$\text{Cellfluorescence} = \frac{I_T - \left(\frac{A_T \times I_B}{A_B}\right)}{N} \quad (1)$$

Where: I_T, total intensity of the image; A_T: total area of the image; I_B, background intensity; A_B, background area; and N, number of cells.

Next, the relative fluorescence intensity was expressed as percentage using the following equation:

$$I\% = \frac{I_{Treat} - I_{NegC}}{I_{Iono} - I_{NegC}} \times 100 \quad (2)$$

Where: I%, relative intensity percentage; I_{Treat}, fluorescence intensity of terpene-treated cells; I_{Iono}, fluorescence intensity of cells treated with ionomycin; and $I_{Neg\ C}$, fluorescence intensity of negative control.

3.3. Statistical analysis

Results are expressed as mean ± standard deviation (SD). All experiments were performed at least in 3 independent assays. Means were compared by One-Way ANOVA followed by the LSD test for post hoc multiple range comparisons. The SPSS Statistics 17.0 statistical package was used for the analyses.

4. Results

4.1. Characterization of terpene-loaded PEG-PLGA NPs

The characteristics of terpene-loaded PEG-PLGA NPs are presented in Table 1. The mean diameter was 218, 262, 354, and 326 nm for blank, MC, CPh and NL NPs, respectively, with a relatively narrow size distribution (PdI < 0.3) for all NPs. A clear correlation could be established between the increase in particle size and the encapsulation efficiency, where the highest EE% was achieved by CPh NPs (60.3%) followed by NL (51.3%) and MC (18.5%) particles. This data emphasizes the effect of terpene properties on loading capacity, since significantly higher loading capacities were achieved with CPh and NL, which have higher molecular weight and are less volatile, compared with MC. The zeta potential of all NPs was within a similar range and around −20 mV.

Table 1
Characteristics of the terpene-loaded nanoparticles (values are the mean ± standard deviation).

Loaded terpene	Mean diameter (nm)	PdI	Zeta Potential (mV)	EE (%)	DL (%)
Blank	217.2 ± 5.6	0.155 ± 0.023	−20.7 ± 1.0	–	–
β–Myrcene	261.5 ± 4.3	0.253 ± 0.019	−20.8 ± 2.1	18.46 ± 0.61	4.78 ± 0.28
β–Caryophyllene	354.9 ± 17.3	0.244 ± 0.009	−19.0 ± 0.7	60.30 ± 2.19	14.32 ± 0.39
Nerolidol	326.7 ± 14.1	0.235 ± 0.028	−19.9 ± 1.5	51.31 ± 2.41	12.54 ± 0.54

4.2. In vitro cytotoxicity

Fig. 2 displays the *in vitro* cytotoxic profiles of free terpenes, blank (drug-unloaded) NPs and terpene-loaded NPs after 24 h incubation with HEK TRPV1 cells. The half maximal inhibitory concentration (IC_{50}) values of all terpene-loaded NPs were approximately 4–5-fold less than that of the corresponding free terpene ($p < 0.001$ for all terpenes). Whereas, when terpenes are compared together, the IC_{50} values of either free or encapsulated terpenes were relatively close and no statistically significant difference was found among the different terpenes. Furthermore, blank PEG-PLGA NPs exhibited negligible cytotoxicity in this cell line at the dilutions corresponding to that of MC-loaded NPs (particles with the lowest EE%). This finding signifies that the cytotoxicity of the terpene-loaded NPs is mainly caused by the encapsulated terpenes, with minimal or no effect from other formulation components.

4.3. Calcium signaling assay

The calcium response of HEK TRPV1 cells against free terpenes, terpenes-loaded PEG-PLGA NPs, and combinations of either free or encapsulated terpenes was explored using a calcium signaling assay. The mean diameter of different NPs dispersed in the assay buffer was similar to that measured in MQ water (blank: 223.4 ± 3.4 nm; MC NPs: 269.7 ± 8.6 nm; CPh NPs: 351.5 ± 4.6, and NL NPs: 334.2 ± 6.3 nm).

4.3.1. Free terpenes vs encapsulated terpenes

Calcium responses of HEK TRPV1 cells to treatment with free terpenes and terpene-loaded NPs are shown in Fig. 3. All free terpenes induced a calcium response, as detected by an increase in the florescence intensity after terpene's addition, and the intensity of response was in the following order: MC > NL > CPh (Fig. 3-A). Furthermore, all nanoparticle formulations significantly increased the intensity of fluorescence in comparison with free terpenes (means of area under the curve [AUC] of MC: $p = 0.013$ [Fig. 3-B]; NL: $p < 0{,}001$ [Fig. 3-C]; and, CPh: $p = 0.006$ [Fig. 3-D]). While CPh displayed the lowest calcium response (both free and NPs) (Fig. 3-D), NL demonstrated an outstandingly remarkable, though delayed, rise in calcium influx when formulated as nanoparticles (Fig. 3-C).

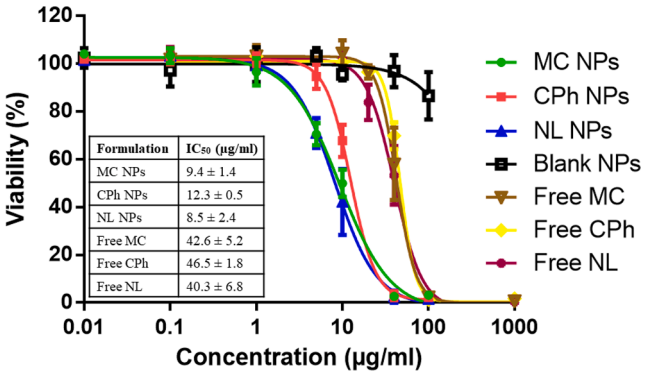

Fig. 2. *In vitro* cytotoxicity of free terpenes, blank (drug-unloaded) NPs, and terpene-loaded NPs in HEK TRPV1 human cells, after 24 h of exposure to a wide range of terpene concentrations (up to 1000 μg/ml). The values are the mean ± SD of triplicate cultures. Cells without treatment were used as control to compute the relative cell viability (%). Insets: IC_{50} values of the terpene-based formulations.

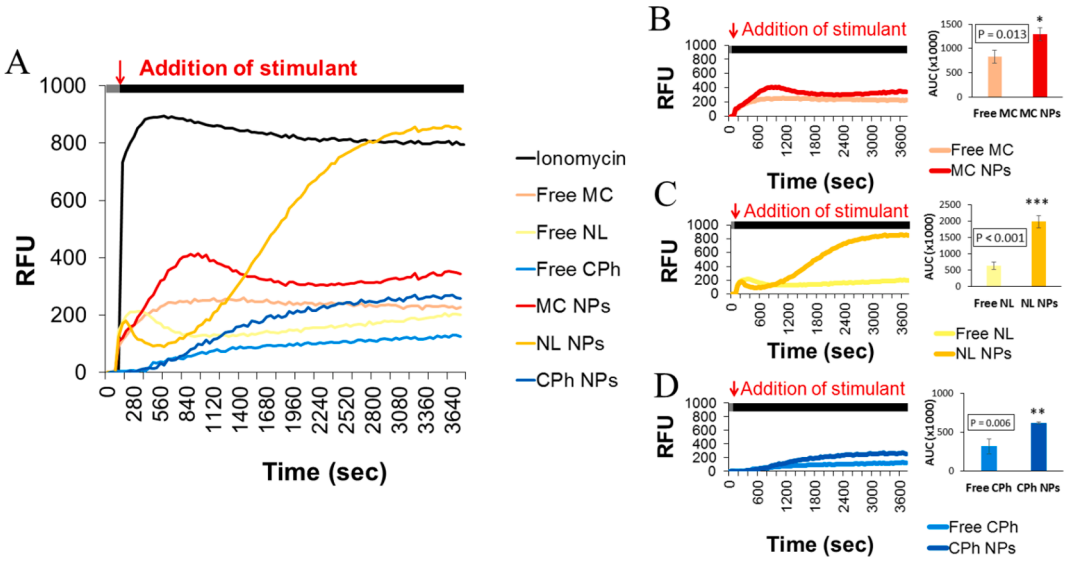

Fig. 3. Fluorescence changes measured using a calcium signaling assay. HEK TRPV1 cells, 15×10^4 cells/well (180 µl), were pre-treated with 1 µM Fluo-4 AM and re-suspended in 1 mM Ca Assay Buffer before the stimulant (free terpenes or terpene-loaded NPs) was added, at a final concentration of 40 µg/ml (20 µl). Ionomycin 4 µM was used as a positive control. Fluorescence was measured over 1 h (one read every 40 sec), at an excitation/emission wavelengths of 485/528 nm. (A) Calcium responses using free and encapsulated terpenes. Calcium responses (left) and corresponding AUCs (right) of: (B) free and encapsulated MC; (C) free and encapsulated NL; and, (D) free and encapsulated CPh. Experiment was performed in triplicate ($n = 3$). Results of calcium responses and AUCs are presented as mean and mean ± SD, respectively. Statistically significant differences are recorded as follows: single asterisk, $p < 0.05$; double asterisk, $p < 0.01$; triple asterisk, $p < 0.001$.

4.3.2. Combinations of free and encapsulated terpenes

Calcium response of HEK TRPV1 cells to combinations of free and encapsulated terpenes was also investigated (Fig. 4). As shown in Fig. 4 (A, B, C and D), in general, all combinations of free terpenes improved the calcium influx in comparison with individual terpenes, and this effect was significant in the combination of MC/NL (Fig. 4-B) and the three terpenes together (MC/NL/CPh; Fig. 4-D). However, no significant enhancement in calcium response was observed when encapsulated terpenes were mixed together (Fig. 4: E, F, G and H). Impressively, it was found that all combinations of NP formulations produced remarkably higher calcium responses when compared to combinations of their respective free terpenes (Fig. 4: I, J, K and L).

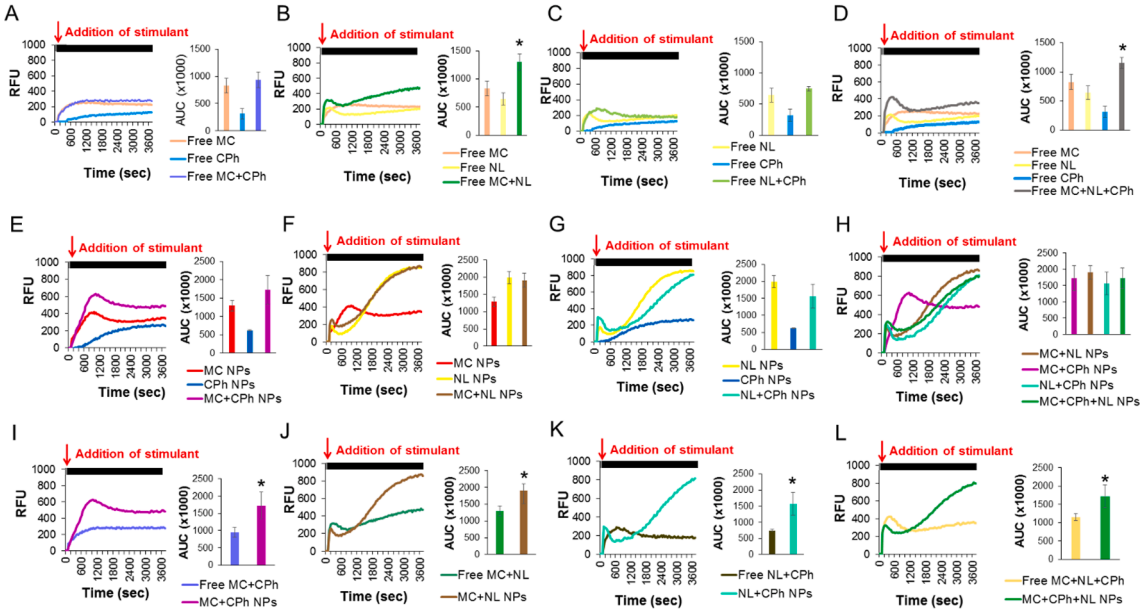

Fig. 4. Calcium responses of individual free terpenes in comparison to their corresponding combinations. Cells, 15×10^4 cells/well (180 µl), were pre-treated with 1 µM Fluo-4 AM and re-suspended in 1 mM Ca Assay Buffer before the stimulant (free terpenes or terpene-loaded NPs) was added, at a final concentration of 40 µg/ml of each terpene (20 µl). Fluorescence was measured over 1 h (one read every 40 sec), at an excitation/emission wavelengths of 485/528 nm. Calcium responses (left) and corresponding AUCs (right) of: (A) Free MC, free NL, and their combination; (B) Free MC, free CPh, and their combination; (C) Free CPh, free NL, and their combination; (D) The three terpenes (free), and their combination. (E) MC NPs, NL NPs, and their combination; (F) MC NPs, CPh NPs, and their combination; (G) NL NPs, CPh NPs, and their combination; (H) NPs of the three terpenes, and their combination; (I) Combinations of free and encapsulated MC and NL; (J) Combinations of free and encapsulated MC and CPh; (K) Combinations of free and encapsulated NL and CPh; and, (L) Combinations of free and encapsulated MC, NL, and CPh. Experiment was performed in triplicate ($n = 3$). Results of calcium responses and AUCs are presented as mean and mean ± SD, respectively. Statistically significant differences are recorded as follows: single asterisk, $p < 0.05$.

4.4. Fluorescence imaging

Fig. 5 shows images of HEK TRPV1 cells 60 min after treatment with assay buffer (A), blank NPs (B), ionomycin (C), free terpenes (D-J), and terpene-loaded PEG-PLGA NPs (K-Q). Fluoresce intensity measured using these images, at 30 and 60 min post treatment, was expressed as relative intensity percentage by comparing all terpenes to the positive control ionomycin (equation (2)). Results are demonstrated in Fig. 6.

In general, all terpenes, both free and encapsulated, promoted the fluorescence intensity compared to non-treated or blank NP-treated cells. In comparison with free terpenes, terpene-loaded NPs induced significantly higher fluorescence intensity, including both single and in-combination terpenes (Fig. 6-A). Based on the induced fluorescence intensity and in accordance with the findings of calcium influx assay, free terpenes showed the following order: MC > NL > CPh; with MC producing a significantly higher intensity than the other two terpenes (Fig. 6-B). However, encapsulated terpenes had a slightly different order (NL > MC > CPh) (Fig. 6-C), where NL NPs produced the highest response ($p < 0.001$) with intensity measuring up to approximately 4-fold and 3-fold that of CPh- and MC-loaded NPs (at 60 min post-treatment), respectively. In addition, MC NPs induced a significantly higher fluorescence intensity in comparison with CPh NPs ($p < 0.05$) (Fig. 6-C).

Additionally, the terpene combinations that produced the highest fluorescence intensity were MC/NL and MC/CPh/NL. These two combinations were effective both in free and encapsulated terpenes and the intensity enhancement was apparent at 60 min post-treatment (Fig. 6-D and E). When images of 30 min and 60 min post-treatment with terpene combinations were compared, only free MC/NL showed a significant increase after 60 min ($p < 0.05$). However, in cells treated with terpene-loaded NPs, all combinations, with an exception of MC/CPh NPs, showed significant rise in intensity at 60 min post-treatment as compared to 30 min post-treatment. Among encapsulated single terpene formulations, a similar significantly increased response was only observed with NL-loaded NPs ($p < 0.001$).

5. Discussion

The terpene-loaded PEG-PLGA NPs were synthesized and tested in HEK cells that express TRPV1. The calcium signaling assay utilized in this work enables the measurement of calcium influx, as a result of TRPV1 activation. Fluorescence intensity changes were monitored using Fluo-4, which was used to measure intra-cellular free Ca^{2+} concentrations (Moriello and De Petrocellis, 2016).

Our work was based on the findings of Jansen et al. who demonstrated that cannabis-derived terpenes, predominantly MC, activate TRPV1 channels inducing calcium fluxes (Jansen et al., 2019). We obtained the HEK TRPV1 cells from the same research group. However, we had to introduce some modifications to the calcium signaling assay developed by Jansen et al. in which a more sophisticated and sensitive instrument (Flexstation 3) was employed. Thus, a higher count of cells (150,000 cell/well in place of 100,000) and higher concentrations of terpenes (MC: 293.6 μM, CPh 195.7 μM, and NL 179.9 μM; compared to up to 30 μM used by Jansen et al) were involved. Similar high concentrations of terpenes have previously been reported in the literature. For example, linalool has been found to activate human TRPA1 at an EC50 of 117 μM (Riera et al., 2009). In addition, the experiment duration was set to 1 h to provide enough time for drug release from NPs and drug interaction with the receptors.

Our results confirm the findings of Jansen et al. regarding free MC, and the relatively small effect of free NL on TRPV1. Moreover, this work demonstrates that the PLGA-based nano-formulations significantly enhance the calcium influx induced by the three terpenes. In general, this improved effect may be explained by the solubilization of the lipophilic terpenes in the core of the nanocapsules, thus improving their ability to interact with the TRPV1 channels. Furthermore, the likely slow drug release, as generally observed for lipophilic substances encapsulated in PEG-PLGA NPs (Rafiei and Haddadi, 2017; Samkange et al., 2019), may explain the time-dependent enhancement of fluorescence intensity shown by the terpene-loaded NPs. Interestingly, NL-loaded NPs demonstrated a two-phase response characterized by a small peak followed by a drastic logistic phase pattern (S curve) reaching a calcium signal similar to that exhibited by ionomycin. In fact, the two-phase response suggests that the generation of calcium signal by the encapsulated NL may be provided by a more complex mechanism. The first small peak may result from the terpene that is released immediately by the nanoparticle formulation followed by a slower but extended release of the terpene. However, as this pattern was not observed by the other two terpenes, it is also possible that the high intercellular concentration of NL achieved by the nano-formulation induces other mechanisms for increasing calcium concentration in the cytosol. One possible mechanism is the mobilization of calcium from endoplasmic reticulum in which functional TRPV1 channels are located and serve as intracellular Ca^{2+} release channels (Gallego-Sandín et al., 2009; Turner et al., 2003). A more in-depth investigation is needed to clarify the mechanism(s) underlying effect induced by NL-loaded NPs, which is not within the

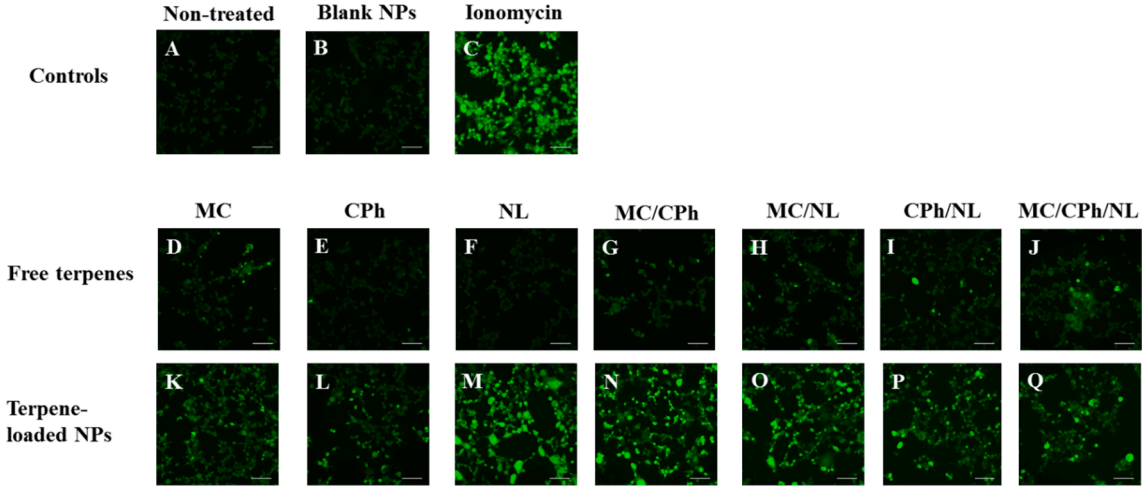

Fig. 5. Fluorescence images of HEK TRPV1 cells acquired using Nikon inverted microscope Eclipse Ti. Cells were pre-incubated with Fluo-4 for 30 min followed by the addition of the stimulant. Images were acquired 60 min after the addition of controls: (A) no treatment, (B) blank NPs, (C) ionomycin; free terpenes: (D) MC, (E) CPh, (F) NL, (G) MC/CPh, (H) MC/NL, (I) CPh/NL, and (J) MC/CPh/NL; and terpene-loaded NPs: (K) MC, (L) CPh, (M) NL, (N) MC/CPh, (O) MC/NL, (P) CPh/NL, and (Q) MC/CPh/NL. Terpenes were used at a concentration of 40 μg/ml. Images are representative of three experiments. Scale bar: 50 μm.

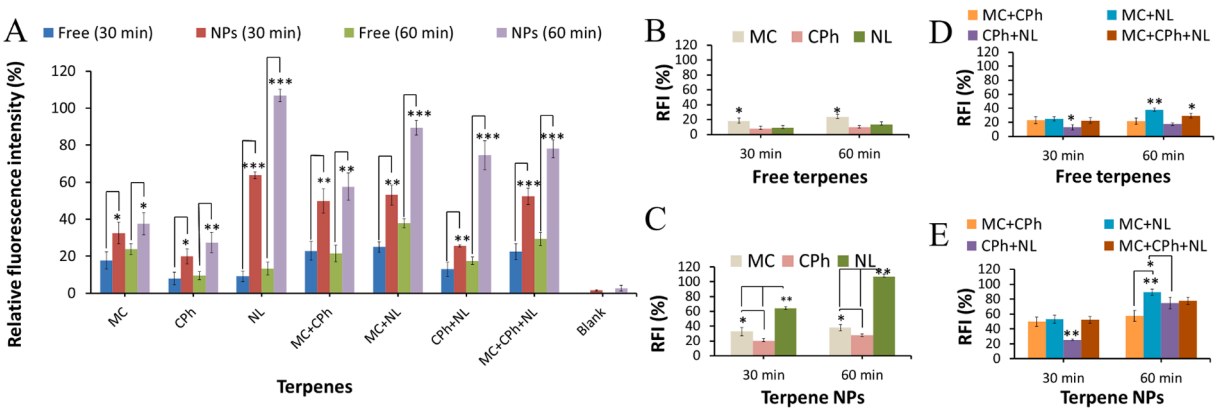

Fig. 6. Relative fluorescence intensity of HEK TRPV1 cells' images acquired 30 and 60 min after treatment with free and encapsulated terpenes. (A) all formulation; (B) individual free terpenes; (C) individual terpene NPs; (D) combinations of free terpenes; and, (E) combinations of terpene NPs. Relative fluorescence intensity was calculated by normalizing the fluorescence intensity of images of terpene-treated cells to that of ionomycin-treated cells. Statistically significant differences are recorded as follows: single asterisk, $p < 0.05$; double asterisk, $p < 0.01$; triple asterisk, $p < 0.001$.

scope of the current work. Moreover, the high-level responses seen by the combinations of the three terpenes may provide an evidence of a synergistic effect.

It is noteworthy that shifts in intracellular Ca^{2+} have been found to promote cell death, through apoptotic or necrotic pathways (Zhai et al., 2020). Therefore, the increased cytotoxicity observed by the encapsulated terpenes in the MTT assay may be explained by the potentially promoted calcium-mediated cell death resulted from the increased intracellular Ca^{2+} concentrations.

In disagreement with our findings, a recent report that tested different terpenoids, including MC (with a concentration up to 30 μM), found that these terpenoids had no activation effect on human TRPV1 (Heblinski et al., 2020). Nevertheless, the discrepant findings may be explained by many variations in the assay conditions, which may include differences in TRPV1expression levels, and variations in the assay method, buffer composition, and experimental temperature used.

Our findings suggest that the newly developed PLGA-based nanosystems can remarkably increase the ability of the tested cannabis-based terpenes to enhance the fluorescence intensity driven by the intercellular calcium ion influx. This effect is correlated with the activation of TPRV1 channels which indicates that the terpene NPs may have great potential for application in pain management.

6. Conclusion

The calcium response of HEK TRPV1 cells against free terpenes, terpene-loaded PLGA-PEG NPs, and combinations of free and encapsulated terpenes was explored using a calcium signaling assay. Whether used individually or in combinations, encapsulated terpenes were found to be superior in improving calcium cellular influx, when compared to free terpenes. The improved activity of the terpenes is believed to be mainly stemmed from solubilization of the terpenes in the core of the nanocapsule and the slow terpene release from the nanosystem. As previously demonstrated by Berrocoso et al. (Berrocoso et al., 2017), it is expected to attain an extended and controlled pain relief after oral administration of these terpene-loaded PLGA-PEG NPs. Further *in vivo* experiments are essential to test the effectiveness of the terpene nanoformulations for pain management, as well as their ability to enhance the bioavailability of the terpenes via oral delivery.

CRediT authorship contribution statement

Mazen M. El-Hammadi: Data curation, Investigation, Methodology, Software, Validation, Visualization, Writing – original draft. **Andrea L. Small-Howard:** Conceptualization, Funding acquisition, Methodology, Project administration, Resources, Writing – review & editing. **Chad Jansen:** Methodology, Resources, Validation, Writing – review & editing. **Mercedes Fernández-Arévalo:** Conceptualization, Funding acquisition, Methodology, Project administration, Resources, Supervision, Validation, Writing – original draft. **Helen Turner:** Methodology, Resources, Validation, Writing – review & editing. **Lucía Martín-Banderas:** Conceptualization, Formal analysis, Funding acquisition, Investigatiom, Methodology, Project administration, Resources, Software, Supervision, Validation, Writing – original draft.

Declaration of Competing Interest

The authors declare that they have no known competing financial interests or personal relationships that could have appeared to influence the work reported in this paper.

Acknowledgements

We specially thank Biology and Spectrophotometry Services from Centro de Investigación, Tecnología e Innovación (CITIUS, Universidad de Seville) for technical assistance.

References

Bautista, D., Julius, D., 2008. Fire in the hole: pore dilation of the capsaicin receptor TRPV1. Nat Neurosci 11 (5), 528–529.
Berrocoso, E., Rey-Brea, R., Fernández-Arévalo, M., Micó, J.A., Martín-Banderas, L., 2017. Single oral dose of cannabinoid derivate loaded PLGA nanocarriers relieves neuropathic pain for eleven days. Nanomedicine 13 (8), 2623–2632.
Booth, J.K., Bohlmann, J., 2019. Terpenes in Cannabis sativa - From plant genome to humans. Plant Sci 284, 67–72.
Bridgeman, M.B., Abazia, D.T., 2017. Medicinal Cannabis: History. Pharmacology, And Implications for the Acute Care Setting P T 42, 180–188.
Brunetti, P., Pichini, S., Pacifici, R., Busardò, F.P., del Rio, A., 2020. Herbal Preparations of Medical Cannabis: A Vademecum for Prescribing Doctors. Medicina 56 (5), 237. https://doi.org/10.3390/medicina56050237.
Bujak, J.K., Kosmala, D., Szopa, I.M., Majchrzak, K., Bednarczyk, P., 2019. Inflammation, Cancer and Immunity-Implication of TRPV1 Channel. Front Oncol 9, 1087.
Burcu, G.B., Osman, C., Asli, C., Namik, O.M., Nese, B.T., 2016. The protective cardiac effects of Beta-myrcene after global cerebral ischemia/reperfusion in C57BL/J6 mouse. Acta Cir Bras 31, 456–462.
Chan, W.-K., Tan, L., Chan, K.-G., Lee, L.-H., Goh, B.-H., 2016. Nerolidol: A Sesquiterpene Alcohol with Multi-Faceted Pharmacological and Biological Activities. Molecules 21 (5), 529. https://doi.org/10.3390/molecules21050529.
Chicca, A., Caprioglio, D., Minassi, A., Petrucci, V., Appendino, G., Taglialatela-Scafati, O., Gertsch, J., 2014. Functionalization of beta-caryophyllene generates novel polypharmacology in the endocannabinoid system. ACS Chem Biol 9, 1499–1507.
Ciftci, O., Oztanir, M.N., Cetin, A., 2014. Neuroprotective effects of beta-myrcene following global cerebral ischemia/reperfusion-mediated oxidative and neuronal damage in a C57BL/J6 mouse. Neurochem Res 39, 1717–1723.

El-Hammadi, M., Arias, J.L., 2015. Advanced engineering approaches in the development of PLGA-based nanomedicines. In: Aliofkhazraei, M. (Ed.), Handbook of Nanoparticles. Springer International Publishing, Switzerland, pp. 1009–1039.

El-Hammadi, M.M., Small-Howard, A.L., Fernández-Arévalo, M., Martín-Banderas, L., 2021. Development of enhanced drug delivery vehicles for three cannabis-based terpenes using poly(lactic-co-glycolic acid) based nanoparticles. Industrial Crops and Products 164, 113345. https://doi.org/10.1016/j.indcrop.2021.113345.

Gallego-Sandín, S., Rodríguez-García, A., Alonso, M.T., García-Sancho, J., 2009. The endoplasmic reticulum of dorsal root ganglion neurons contains functional TRPV1 channels. J Biol Chem 284 (47), 32591–32601.

Gee, K.R., Brown, K.A., Chen, W.-N.-U., Bishop-Stewart, J., Gray, D., Johnson, I., 2000. Chemical and physiological characterization of fluo-4 Ca(2+)-indicator dyes. Cell Calcium 27 (2), 97–106.

Han, L., Fu, Y., Cole, A.J., Liu, J., Wang, J., 2012. Co-encapsulation and sustained-release of four components in ginkgo terpenes from injectable PELGE nanoparticles. Fitoterapia 83 (4), 721–731.

Heblinski, M., Santiago, M., Fletcher, C., Stuart, J., Connor, M., McGregor, I.S., Arnold, J. C., 2020. Terpenoids Commonly Found in Cannabis sativa Do Not Modulate the Actions of Phytocannabinoids or Endocannabinoids on TRPA1 and TRPV1 Channels. Cannabis and cannabinoid research 5 (4), 305–317.

Huang, J., Liu, J., Qiu, L., 2020. Transient receptor potential vanilloid 1 promotes EGFR ubiquitination and modulates EGFR/MAPK signalling in pancreatic cancer cells. Cell Biochem Funct 38 (4), 401–408.

Iannitelli, A., Grande, R., Stefano, A.D., Giulio, M.D., Sozio, P., Bessa, L.J., Laserra, S., Paolini, C., Protasi, F., Cellini, L., 2011. Potential antibacterial activity of carvacrol-loaded poly(DL-lactide-co-glycolide) (PLGA) nanoparticles against microbial biofilm. Int J Mol Sci 12 (8), 5039–5051.

Jansen, C., Shimoda, L.M.N., Kawakami, J.K., Ang, L., Bacani, A.J., Baker, J.D., Badowski, C., Speck, M., Stokes, A.J., Small-Howard, A.L., Turner, H., 2019. Myrcene and terpene regulation of TRPV1. Channels (Austin) 13 (1), 344–366.

Jara-Oseguera, A., Simon, S., Rosenbaum, T., 2008. TRPV1: on the road to pain relief. Curr Mol Pharmacol 1 (3), 255–269.

Maharajan, M.K., Yong, Y.J., Yip, H.Y., Woon, S.S., Yeap, K.M., Yap, K.Y., Yip, S.C., Yap, K.X., 2020. Medical cannabis for chronic pain: can it make a difference in pain management? Journal of Anesthesia 34 (1), 95–103.

Marongiu, L., Donini, M., Bovi, M., Perduca, M., Vivian, F., Romeo, A., Mariotto, S., Monaco, H.L., Dusi, S., 2014. The inclusion into PLGA nanoparticles enables α-bisabolol to efficiently inhibit the human dendritic cell pro-inflammatory activity. Journal of Nanoparticle Research 16, 2554.

Molinas, A.J.R., Desmoulins, L.D., Hamling, B.V., Butcher, S.M., Anwar, I.J., Miyata, K., Enix, C.L., Dugas, C.M., Satou, R., Derbenev, A.V., Zsombok, A., 2019. Interaction between TRPV1-expressing neurons in the hypothalamus. Journal of neurophysiology 121 (1), 140–151.

Moriello, A.S., De Petrocellis, L., 2016. Assay of TRPV1 Receptor Signaling. Methods Mol Biol 1412, 65–76.

Rafiei, P., Haddadi, A., 2017. Docetaxel-loaded PLGA and PLGA-PEG nanoparticles for intravenous application: pharmacokinetics and biodistribution profile. Int J Nanomedicine 12, 935–947.

Riera, C.E., Menozzi-Smarrito, C., Affolter, M., Michlig, S., Munari, C., Robert, F., Vogel, H., Simon, S.A., le Coutre, J., 2009. Compounds from Sichuan and Melegueta peppers activate, covalently and non-covalently, TRPA1 and TRPV1 channels. Br J Pharmacol 157 (8), 1398–1409.

Romero-Sandoval, E.A., Fincham, J.E., Kolano, A.L., Sharpe, B.N., Alvarado-Vázquez, P. A., 2018. Cannabis for Chronic Pain: Challenges and Considerations. Pharmacotherapy 38 (6), 651–662.

Russo, E.B., 2011. Taming THC: potential cannabis synergy and phytocannabinoid-terpenoid entourage effects. Br J Pharmacol 163, 1344–1364.

Samkange, T., D'Souza, S., Obikeze, K., Dube, A., 2019. Influence of PEGylation on PLGA nanoparticle properties, hydrophobic drug release and interactions with human serum albumin. J Pharm Pharmacol 71 (10), 1497–1507.

Sharma, C., Al Kaabi, J.M., Nurulain, S.M., Goyal, S.N., Kamal, M.A., Ojha, S., 2016. Polypharmacological Properties and Therapeutic Potential of beta-Caryophyllene: A Dietary Phytocannabinoid of Pharmaceutical Promise. Curr Pharm Des 22, 3237–3264.

Small-Howard, A.L., Martín-Banderas, L., El-Hammadi, M.M., Fernández-Arévalo, M., 2019. Therapeutic nanoparticles encapsulating terpenoids and/or cannabinoids. WO2020094908A1.

So, C.L., Milevskiy, M.J.G., Monteith, G.R., 2020. Transient receptor potential cation channel subfamily V and breast cancer. Lab Invest 100 (2), 199–206.

Turner, H., Fleig, A., Stokes, A., Kinet, J.P., Penner, R., 2003. Discrimination of intracellular calcium store subcompartments using TRPV1 (transient receptor potential channel, vanilloid subfamily member 1) release channel activity. Biochem J 371, 341–350.

Yang, F., Zheng, J., 2017. Understand spiciness: mechanism of TRPV1 channel activation by capsaicin. Protein Cell 8 (3), 169–177.

Zhai, K., Liskova, A., Kubatka, P., Büsselberg, D., 2020. Calcium Entry through TRPV1: A Potential Target for the Regulation of Proliferation and Apoptosis in Cancerous and Healthy Cells. Int J Mol Sci 21 (11), 4177. https://doi.org/10.3390/ijms21114177.

Zheng, W., Wen, H., 2019. Heat activation mechanism of TRPV1: New insights from molecular dynamics simulation. Temperature (Austin) 6 (2), 120–131.